CHAPTER 1

Review of deNO$_x$ Technology for Mobile Applications

T. V. JOHNSON* AND A. JOSHI

Corning Incorporated, HP-CB-2-1, One Museum Way, Corning, NY 14831, USA
*Email: JohnsonTV@Corning.com

1.1 Introduction

NO_x is formed when air is heated to very high temperatures, and is thus emitted from combustion and engines. The most prevalent NO_x species from engines is NO. It will oxidize in the atmosphere to form NO_2, and also react with most hydrocarbons to form ozone; both ozone and NO_2 are strong oxidants and toxic. Thus NO_x is a criteria pollutant and is regulated.

NO_x is very-effectively controlled from gasoline engines with three-way catalysts (CO, hydrocarbons, NO_x), but they only operate under stoichiometric conditions. In the presence of excess oxygen, CO and hydrocarbon react with it rather than chemically reduce the NO_x. For lean conditions, selective catalytic reduction (SCR) is the leading method of remediation. The reductant, ammonia (NH_3), which generally needs to be added to the exhaust, selectively reduces the NO_x rather than being oxidized by the excess oxygen, like in the case of innate exhaust reductants, CO and hydrocarbons. NO_x trap catalysts[†] (NTCs) can also be effective in reducing NO_x. During lean conditions the NO_x is stored as a nitrate in the catalyst, and then in periodic

[†]NO_x trap catalysts are also commonly referred to by other names, like lean NO_x trap (LNT), NO_x storage catalyst (NSC), and NO_x storage and reduction (NSR) catalyst.

Catalysis Series No. 33
NO_x Trap Catalysts and Technologies: Fundamentals and Industrial Applications
Edited by Luca Lietti and Lidia Castoldi

Published by the Royal Society of Chemistry, www.rsc.org

rich conditions the nitrate dissociates releasing the NO_2, with is reduced by CO or hydrocarbon reductant in the absence of oxygen. A subset of these is the passive NO_x adsorber (PNA), which generally stores NO_x as a nitrite at low temperatures ($<200\ ^{\circ}C$) and releases the NO at higher temperatures.

In this introductory chapter a general outlook at the emission limits for both diesel and gasoline engines will be reported, along with general engine trends, and the actual aftertreatment technologies used for both types of engines. Future perspectives in the field of lean NO_x abatement might also be enlightening. This chapter is not intended to be all-encompassing and comprehensive. Representative papers and presentations were chosen to provide examples of new, key developments and direction. For a more detailed review of emissions and engine technologies, the reader is referred to the authors' last five review papers.[1–5]

1.2 Regulatory Overview

Although the first commercial lean deNO_x system was a NTC coated onto a diesel particulate filter (DPF) on the European Toyota Avensis diesel in the early 2000s, and then separate NTC on the US Dodge Ram diesel truck (Cummins engine) as a separate unit in 2007, the first wide-scale use of lean deNO_x was the implementation of SCR for heavy-duty (HD) truck applications in Europe in 2005 to meet the Euro IV HD regulations. The US Tier 2 and California LEVII (Low Emission Vehicle) light-duty regulations were the first to require lean NO_x control on light-duty (LD) applications, beginning in 2007, in which VW used only an NTC; BMW used SCR; and Mercedes used both an LTC and ''passive'' SCR (NH_3 generated by the upstream LTC during rich periods) in addition to SCR on some models. Mercedes is the only automaker to make a lean-burn gasoline vehicle, for the European market. It uses two NTCs in a series architecture. SCR did not make its way into nonroad (NR) applications until 2011 in both the USA and Europe. NTCs were not widely used in Europe until the LD Euro 6 regulations started in 2014.

Following is a general overview of the LD and HD regulations pertinent to understanding the main drivers for NO_x control systems.

1.2.1 Light-duty Regulations

The leading light-duty diesel and gasoline non-methane hydrocarbon and NO_x regulations are graphically shown in Figure 1.1. Only the USA (Federal and California LEVIII) has the dynamometer test-cycle and limit value combination to force NO_x aftertreatment on diesel engines. All require a diesel particulate filter (regulations not shown). However, many of Euro 6 applications have NO_x aftertreatment to minimize NO_2 emissions and fuel consumption.

Starting in September 2017 all new diesel platforms and in September 2019 all new diesel vehicles will need to meet an additional layer of NO_x tailpipe regulations called RDE (real driving emissions). As part of their type

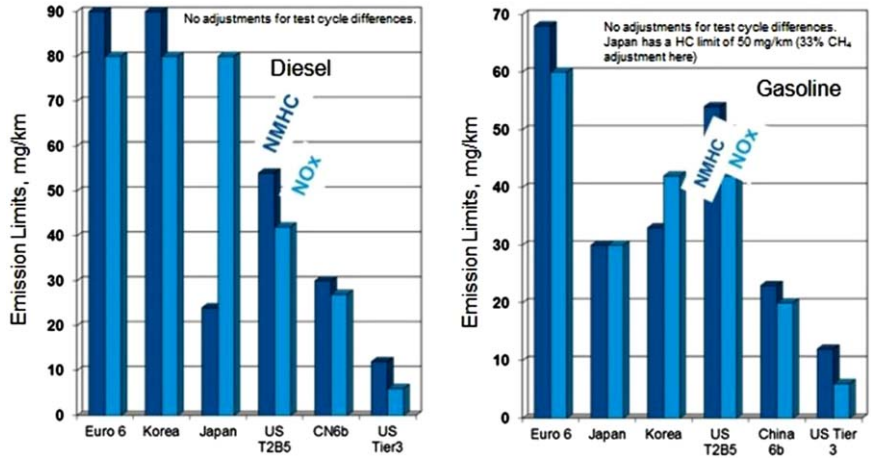

Figure 1.1 Leading light-duty diesel and gasoline NO_x and non-methane hydrocarbon emissions. China 6b begins in 2023 and US Tier 3 is phasing-in 2017 through 2025. All other regulations are currently being enforced.

approval testing (and over the regulatory life of the vehicle), vehicles are equipped with PEMS (portable emissions measurement systems) and driven on routes that meet certain specifications. The data are analyzed using two different protocols.[6] NO_x levels need to be below the RDE limits of 168 mg km^{-1} (2.1× the dynamometer limit value). In January 2020 and 2021 (new platforms, and all new vehicles, respectively) the RDE NO_x limits drop to 120 mg mile^{-1} (1.5× dynamometer limits). These two additional regulations require more NO_x control either through improved calibration or more hardware.

1.2.2 Heavy-duty Truck Regulations

Figure 1.2 shows a summary of the key heavy-duty (HD) truck regulations in the world, along with estimates of the best commercially-viable engine-out NO_x and PM capabilities as measured on the European Steady-state Cycle (ESC). The first vehicle regulation in the world that was attained with SCR systems was the Japan 2005 HD truck regulation in October 2004, shortly followed by Euro IV in January 2005. Although Euro IV was only a 30% NO_x tightening from Euro III (2000), the PM (particulate matter) regulation dropped ~80%, and truck manufacturers generally elected to tune their engines for higher NO_x and lower PM and fuel consumption, and then use SCR to drop the tailpipe levels to within the NO_x (and PM) requirements. Interestingly, although the US2007 NO_x regulations were 60% lower than for Euro IV, and the PM regulations were about 35–55% tighter (steady state and transient testing, respectively), the US manufacturers chose to meet the NO_x regulations with engine technology (mainly exhaust gas recirculation, EGR), and the PM regulations with diesel particulate filters (DPFs). The Japan 2005

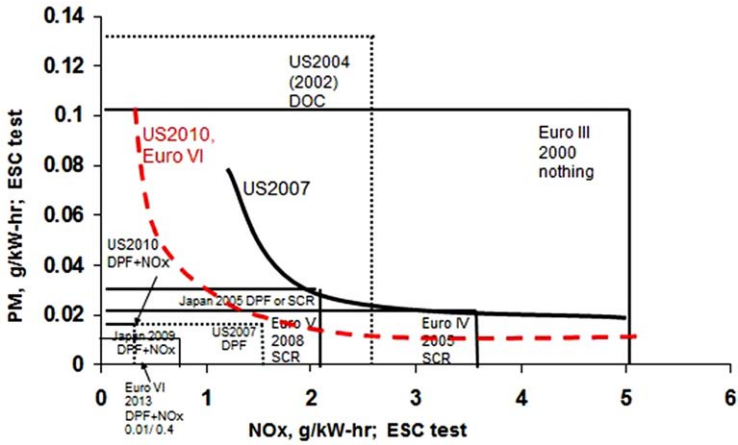

Figure 1.2 Overview of key HD tailpipe regulations as measured on the European Steady-state Cycle (ESC). The dashed and solid lines represent an estimate of engine-out emissions for engines in 2007 and for meeting the US2010 and Euro VI regulations.

regulation is intermediate between Europe and the US for both NO_x and PM, and there was a split of approaches used in Japan, with trucks in high fuel consumption applications generally using a European SCR-only approach, and all others using a EGR + DPF approach.

In the 2009+ timeframe, Japan 2009, US2010, and Euro VI (2013) all require both SCR and DPF solutions. These regulations range from 0.26 to 0.7 g NO_x kW-h^{-1} and 0.010 to 0.013 g PM kW-h^{-1}. In 2016 India finalized their Bharat VI regulations, which are nearly identical to Euro VI, for implementation in April 2020. In late 2016 China proposed their China VI regulations, which deviate from Euro VI by requiring remote-transmission OBD (on-board diagnosis; signals sent to authorities) of key emissions components, higher altitude real-world testing, and some chassis dynamometer testing.

HD NO_x regulations are tightening further, with California taking the lead.[1,2] They are now evaluating the feasibility of cutting NO_x by about 90% from 0.260 g kWh^{-1} by 2024.

1.3 Emission Control Technology for Diesel and Gasoline Engines

Emission control systems were for used on gasoline-fueled vehicles in 1975 to meet the US Clean Air Act requirements. These were simple oxidation catalysts by today's standards, and achieved about 70% conversion of CO and hydrocarbons. Forty years later gasoline emission control systems are achieving 99.5% conversion of hydrocarbons, CO, and NO_x. The first commercial vehicular SCR systems date to 2013, and fourteen years later are

achieving 99% NO_x conversion under high-load conditions ($T > 250$ °C). The first NTC systems in volume came in 2007, and achieved 70–75% conversion. Due to high temperature efficiency issues, the best accomplish perhaps 85–90% NO_x conversion over many driving conditions, but when combined with SCR the system can achieve 95% NO_x conversion over a range of conditions.

For particulate control, wall-flow filters are the norm. They started out uncoated for diesel applications, and quickly migrated to incorporating an oxidation catalyst (platinum) coating. Now in light-duty and some non-road applications filters are coated with SCR catalyst, but none have a NTC catalyst like in the very first lean NO_x control commercial system. Diesel particulate filters drop fine particulates by 2–3 orders of magnitude. Gasoline particulate filters are also now commercialized, but contrary to the diesel case, both TWC-coated and uncoated filters are emerging together.

The next sections will discuss the state-of-the-art for all these systems.

1.3.1 Selective Catalytic Reduction (SCR)

SCR systems are by far the leading type of system for reducing NO_x because they have the best efficiency. This allows heavy-duty engines to be calibrated for higher NO_x and better fuel efficiency and yet meet the emissions standards. This section will generally describe the key aspects of SCR deNO$_x$, and discuss some of the latest information on critical aspects.

SCR systems use ammonia to selectively reduce the NO_x on special catalysts. The ammonia comes from a urea solution whereby, when it is sprayed into the exhaust before the SCR catalyst, the urea decomposes in two steps to form ammonia (in addition to water and CO_2).

The chemistry of SCR systems is quite complex, with many different types of reactions:

$$NH_3 + NO + \tfrac{1}{4}O_2 \rightarrow N_2 + \tfrac{3}{2}H_2O \quad (1.1)$$

$$NH_3 + \tfrac{1}{2}NO + \tfrac{1}{2}NO_2 \rightarrow N_2 + \tfrac{3}{2}H_2O \quad (1.2)$$

$$NH_3 + \tfrac{3}{4}NO_2 \rightarrow \tfrac{7}{8}N_2 + \tfrac{3}{2}H_2O \quad (1.3)$$

Not shown are the urea decomposition reactions that form the ammonia. Reaction (1.1) is generally the ''standard SCR reaction''. As NO_2 is always present in the exhaust to some extent (maybe 10% of NO_x), Reaction (1.2) is also pertinent, and is the fastest and preferred NO_x reduction reaction, especially at low temperatures. To promote this ''fast SCR reaction'' a DOC (diesel oxidation catalyst) is commonly used to form NO_2 over platinum by the following reaction:

$$NO + \tfrac{1}{2}O_2 \rightarrow NO_2 \quad (1.4)$$

If too much NO_2 is produced in the DOC, more than $1:1 = NO:NO_2$, then reaction (1.3), the slowest NO_x reduction reaction, becomes operative. This is

undesirable because the ''excess'' NO_2 can yield N_2O, which is a strong greenhouse gas:

$$NH_3 + NO_2 \rightarrow \tfrac{1}{2}N_2 + \tfrac{1}{2}N_2O + \tfrac{3}{2}H_2O \quad (1.5)$$

If the reactants are not well-mixed, if excess ammonia is injected to obtain high $deNO_x$ efficiencies, or if ammonia stored on the SCR catalyst is released too fast, ammonia emissions can occur. To remediate this, an ammonia slip catalyst (ASC) is utilized after the SCR catalyst to oxidize the excess ammonia:

$$NH_3 + \tfrac{3}{4}O_2 \rightarrow \tfrac{1}{2}N_2 + \tfrac{3}{2}H_2O \quad (1.6)$$

If ammonia oxidation is incomplete, N_2O can form from ammonia:

$$2NH_3 + 2O_2 \rightarrow N_2O + 3H_2O \quad (1.7)$$

And, if both NO and NH_3 are present in a slip catalyst with no SCR catalyst, the following reaction occurs:[7]

$$NO + NH_3 + \tfrac{3}{2}O_2 \rightarrow N_2O + \tfrac{3}{2}H_2O \quad (1.8)$$

To meet the current US2010 (HD) and Euro VI regulations, cycle-average $deNO_x$ efficiencies approaching 98% are realized. High $deNO_x$ efficiencies allow more fuel-efficient higher engine-out NO_x calibrations. Efficiencies in the light-duty sector are 90–95% due to the lower temperatures. Work is continuing in the USA to go even higher in efficiency to meet the current and emerging Tier 3 light duty (LD) NO_x regulations.

There are generally three types of SCR catalysts utilized commercially, copper zeolites, iron zeolites, and vanadia. Zimmermann *et al.*[8] summarizes the attributes of these, plus an experimental mixed metal oxide (MMO) catalyst, in Figure 1.3.

Copper zeolites have innate catalytic oxidation capability, so they form NO_2 by reaction (1.4) without a DOC. This favors the fast SCR reaction (1.2) at lower temperatures and reduces NO_2 sensitivity. Henry[9] shows that despite 2× more precious metal on the DOC in the vanadia system, a copper zeolite with 30% less volume has half of the cumulative NO_x emissions on a hot WHTC. A 25% smaller SCR catalyst results in 20% less mat, 60% less insulation, and 40% less stainless steel. Conversely, they also oxidize NH_3 (reaction (1.6)), slightly decreasing their effectiveness at higher temperatures. At lower temperatures, ammonia can oxidize over copper zeolites by reaction (1.7) to form N_2O.

Vanadia has much better sulfur tolerance, giving it favor in developing markets.[10] These systems are susceptible to ammonia sulfate/bisulfate blinding[11] at lower temperatures (200–300 °C), but are not otherwise affected much by sulfur. However, Kumar *et al.*[12] show NO_2 from the DOC is compromised by sulfur. After 12 h of exposure to 20 ppm SO_2, the NO_2 make of a DOC at 250 °C dropped from 40% to 12%. It is reasonable to assume that this would impair the vanadia SCR system performance. For copper zeolites, the effect is on the SCR performance itself. Upon saturation exposure to

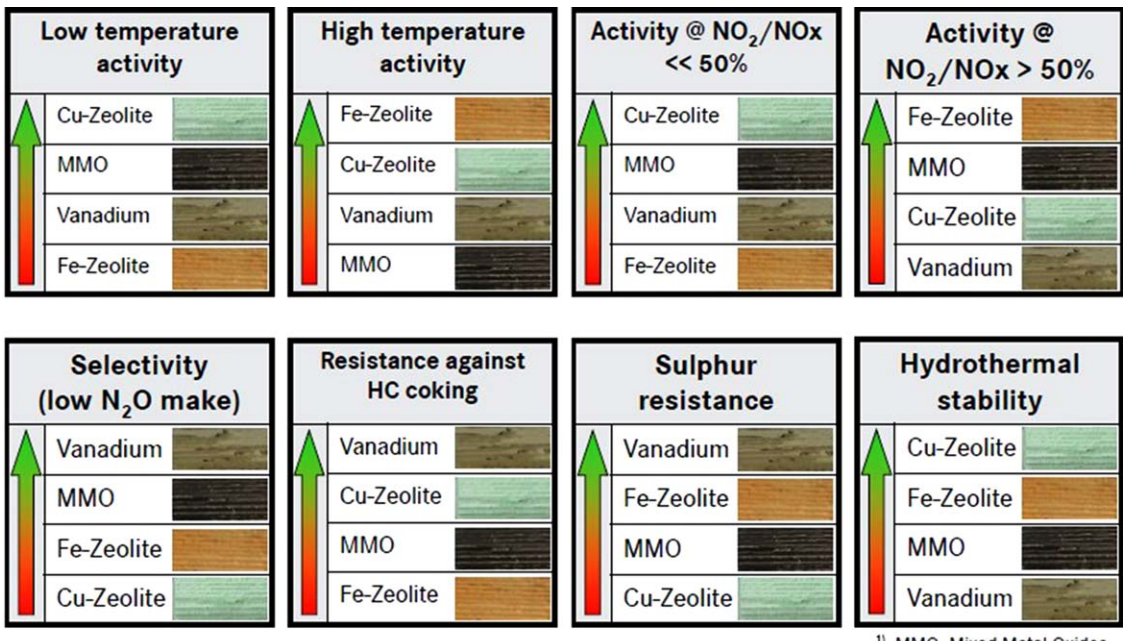

Figure 1.3 Ranking of SCR catalysts for various important attributes.
Reprinted with permission of SAE International, from F. Zimmermann, U. Gärtner, P. Benz, M. Ernst and J. Lehmann, presented at SAE Heavy Duty Emission Control Symposium 2014, Göteborg, 17–18 September 2014, Copyright © 2014.

sulfur at 200 °C, the deNO_x efficiency at 220 °C of the copper zeolite drops from 100% to 80%, but recovers fully after 30 min at 500 °C. The sulfur effect is worse at sulfation exposures of 400 °C. However, most notably the sulfur impacts are diminished when NO_2 is used to enhance NO_x conversion at lower temperatures. A fully sulfated copper zeolite with 40% NO_2 make is only 15% less efficient for deNO_x at 245 °C than a clean one. Further, Kumar *et al.*[13] show that desulfation of copper zeolites is accelerated and temperatures reduced if a reductant is used. Excess ammonia is one such reductant.

Improved copper zeolite SCR catalyst formulations are emerging. The most thermally stable copper zeolite formulations in the market today are stable to about 800 °C. Ryu *et al.*[14] developed a copper zeolite that shows comparatively little deterioration after 12 h of exposure at 900 °C. Compared to the best commercial catalysts today, the new copper zeolite also has similar or lower N_2O emission and less high-temperature ammonia oxidation, resulting in excellent NO_x conversion to about 550 °C. Sulfur tolerance is similar to others but its release is easier, with full recovery after desulfation at 500 °C for 2 h. In another approach, Gao *et al.*[15] used Na additions to copper zeolite to increase the high temperature performance.

As shown in Figure 1.3, vanadia catalysts have poor high-temperature durability due to sublimation of vanadia and tungsten. Liu *et al.*[16] studied vanadia and tungsten release from a commercial SCR catalyst using a bench and engine-based method. They found vanadia emissions on the engine method were always higher, as much as 3× higher at 500 °C, but only 1.5× higher at 700 °C. The engine-based approach clearly provides a more complete measurement of metal emissions, especially at lower temperatures where the dominant release mechanism may not be the thermal/chemical route. This is most likely because the engine-based approach can measure particle-phase and particle-bound vapor-phase metal emissions which are adsorbed onto particulate matter. The trends measured on the bench reactor are similar and the results within the same order of magnitude, so the authors contend the laboratory method is satisfactory for qualitative assessment, but the cost is much lower. They found new catalysts are much more durable, with no emissions at 500 °C and two orders of magnitude lower emissions at 600 °C. Even so, vanadia catalysts are not used in LD applications as HT DPF (diesel particulate filter) regeneration is commonly used and can expose the SCR catalyst to much higher temperatures.

N_2O emissions from SCR catalysts is becoming better understood and remediated. Jansson *et al.*[17] looked at the tradeoff between ammonia NO_x ratio (ANR), NO_x removal, and N_2O formation for vanadia, and copper and iron zeolite, catalyst systems. Figure 1.4 shows the N_2O–NO_x tradeoff for the three catalysts measured for full systems on the WHTC (European World-Harmonized Heavy-Duty Transient Cycle). The precious metal loading of the DOCs varied to suit the needs of the catalyst, and the same high selectivity ASC (ammonia slip catalyst) was used. With increasing ANR (ammonia NO_x ratio) the tailpipe NO_x drops until a critical ANR is reached whereby N_2O

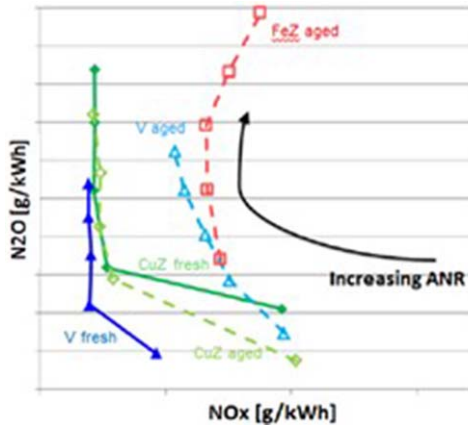

Figure 1.4 N_2O, NO_x, and ANR (ammonia to NO_x ratio) tradeoff for fresh and aged catalysts. N_2O is created when the excess NH_3 is partially oxidized. Aged Cu zeolites have the best tradeoff, and further optimization can improve both the vanadia and copper zeolites.
Reprinted with permission of SAE International, from "Heavy Duty Emission Control System Analysis and Optimization for Future Demands", J. Jansson, Å. Johansson, H. Sjovall, M. Larsson, G. Smedler, C. Newman and J. Pless, *SAE Technical Paper*, 2015, 2015-01-0997, Copyright © 2015.

begins to form with little further NO_x reduction, The fresh vanadia catalyst exhibits the best tradeoff, but deteriorates with aging (100 h at 580 °C). For aged catalysts, the Cu-zeolite exhibits the best performance. With further optimization of the DOC precious metal loading (more NO_2 for the vanadia, less for the copper zeolite), both systems delivered good performance. The iron-zeolite could not deliver low NO_x without high N_2O. The investigators also looked at the linear layout architecture, and compared this to the muffler box configuration. NO_x emissions are the same on the WHTC, but are higher for the linear design in the colder portions of the cycle, and higher for the box design at the hotter portions when NH_3 is oxidized.

Understanding NH_3 adsorption behavior is fundamental to extending SCR efficiency, especially at low temperatures. Partridge *et al.*[18] did an interesting fundamental study on the NH_3 storage distribution in an SCR catalyst as a function of temperature, gaseous ammonia concentration, and NO_x levels. They found that the dynamic capacity, when NO_x is present, deviated from the total capacity in the axial direction, and that the departure correlates to the knee of the Langmuir adsorption isotherm (in the Langmuir model, adsorption increases with gas concentration, but then tapers off at higher gas concentrations). From this and other results, the authors deduce that ammonia adsorption kinetics are faster than the SCR reaction.

SCR catalyst systems will age, and this impacts NH_3 capacity. Bartley *et al.*[19] describe NH_3 storage capacity as a function of SCR catalyst aging time and temperature. The researchers modeled the aging using first-principle

Langmuir adsorption isotherms. These data can be used in model-based control algorithms to calculate the current NH_3 storage capacity of an SCR catalyst operating in the field, based on time and temperature history.

SCR catalysts are now being incorporated into DPFs, especially in LD applications. This saves space and positions the catalyst closer to the engine for hotter temperatures for significant benefits in LD applications. However, Kojima *et al.*[20] shows that the SCR catalyst utility is decreased. When comparing a flow-through SCR catalyst to a DPF coated with the same but decreased amount of SCR catalyst, the filter geometry gives 10–20% lower relative deNO_x efficiencies in isothermal testing from 175 to 325 °C, and 20% relative reduced efficiency on the US LD cycle. To improve light-off performance even more, a small flow-through SCR catalyst was added in front of the DPF-SCR. In addition to lower SCR catalyst loadings, reduced utility of the catalyst, and soot consuming NO_2 that would otherwise promote the fast SCR reaction, Yang *et al.*[21] found that if the soot penetrates into the wall, as in the early stages of filtration, it can blind the SCR catalyst and deteriorate deNO_x performance. However, Mihai *et al.*[22] show that for the fast SCR reaction, at temperatures starting from 150 °C, the activity was significantly higher in the presence of soot. Soot is thought to inhibit ammonium nitrate formation, as CO_2 production at low temperature was observed and N_2O, a product of ammonium nitrate decomposition, was less in the presence of soot.

SCR system control is becoming more important as system deNO_x efficiencies increase. This usually involves NH_3 storage and overdosing, and control of ammonia slip especially in transient conditions. Model-based control is the leading emerging approach for doing this. Iivonen and Wabnig[23] describe a system controller that incorporates observer and controller models. The result is reduced calibration time, reduced emissions at any given ammonia slip level, use of off-line calibration, and reduced hardware costs. Chavannavar[24] provided some insight into their approach wherein NO_x conversion and NH_3 slip over a given transient cycle can be tuned by the ''slip factor'', which is used in SCR Offset Controller.

1.3.2 NO_x Trap Catalysts

NO_x trap catalysts are currently the leading deNO_x concept for the smaller lean-burn (diesel, direct injection gasoline) passenger cars due to limited space for a large SCR system (including the urea tank) or if less deNO_x efficiency is needed. The deNO_x efficiency is nominally 70–80%, much lower than that of the next generation SCR system at 95+%, and the precious metal usage is high (~10–12 g for a 2 liter engine). As a result, efforts are focused on improving efficiency while reducing precious metal usage. In addition, as they store NO_x in the form of a nitrate, they also store sulfur as sulfates. These are more stable than nitrates and significantly deteriorate NO_x performance.

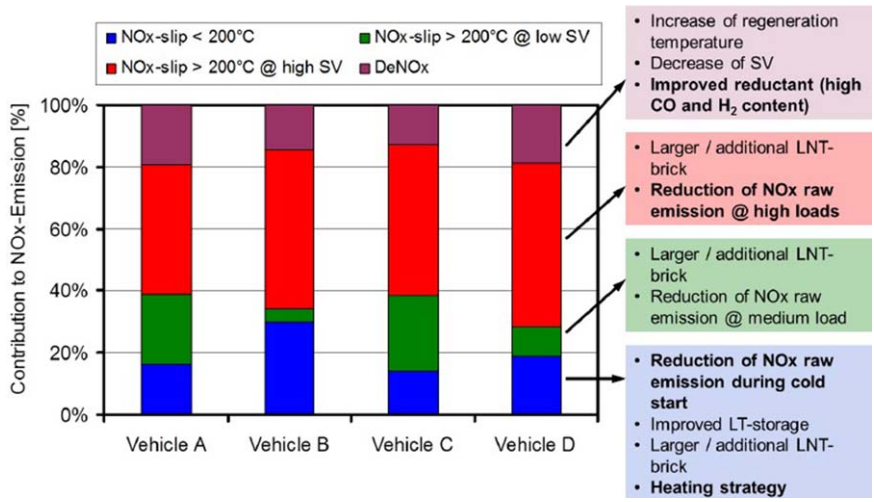

Figure 1.5 Operational sources of NO_x emissions from four vehicles equipped with LNTs.
Reprinted with permission from Achieving LEV III with a Light-Duty Diesel Powertrain – Impossible or Challenging? D. Tomazic and H. Nanjundaswamy, presentation at the 4th International CTI Conference on NO_x Reduction – Current and Future Solutions for On- and Off-Road Applications, Detroit, June 2012.

Tomazic and Nanjundaswamy[25] identified the gaps in NO_x control using NTCs. Figure 1.5 shows the sources of NO_x emissions for four different vehicles equipped with an NTC. On the order of 55–75% of the NO_x slip occurs during operating points when the NTC is functional ($T > 200$ °C, medium to high space velocities). Cold start or low temperature operation accounts for 15–30% of the emissions.

Much of the issue on NO_x slip is related to NTC size and platinum group metal (PGM) loading, so technologies that can reduce PGM loadings through improved utilization are key to LNT improvement. Researchers at Nissan used a selective PGM deposition process to enhance precious metal dispersion.[26] The concept is to use a surfactant to preferentially apply the platinum to the ceria rather than to the alumina in the washcoat. Upon aging, the grain growth of platinum is greatly reduced because the small ceria grains limit the growth. Precious metal usage is cut 50% without compromise in NO_x emissions. The researchers also have identified that the NO_x desorption rate is considerably slower than adsorption or catalyst reactions at low temperature. NO_x desorption rate is increased by enhancing contact of ceria and baria, the NO_x trapping material. Work is continuing to verify the effect.

Umeno *et al.*[27] described an improved LNT with higher sulfur tolerance. The main NO_x adsorbing material, barium oxide (baria), is supported on one basic material, and strontium oxide, which acts as a scavenger for the sulfur to protect the baria, is coated in the whole catalyst with high dispersion.

In bench testing the NO_x removal efficiency of the new catalyst is 2× that of a standard baria LNT at a 3 g L^{-1} sulfur loading. The sulfur is also released at a higher rate and at lower temperatures.

Li *et al.*[28] did fundamental work on LNT using both cyclic operation and temperature-programmed rich NO_x reduction. The results consistently showed substantially better performance when the rhodium was in the reduced state rather than in the oxidized state. NO_x slip can occur during the transition from oxidized to reduced state. Kinetics analyses indicate that NO reduction over the reduced catalyst is first order dependent on NO inlet concentration with an apparent activation energy of 180 ± 14 kJ mol^{-1}, which is independent of aging or the type of reductant.

One of the more interesting NTC developments in recent years is from Toyota, wherein they significantly improve HT performance by oscillating the air : fuel ratio in the lean regime to achieve much better NO_x removal.[29] Subsequent reports,[30,31] describe more of the underlying fundamentals and system optimization. Fundamentally, as depicted in Figure 1.6, at high temperatures (>450 °C) hydrocarbons reduce NO_x more effectively than hydrogen and CO in lean conditions, which preferentially react more with oxygen than with NO_x. Conditions that enhance the utility of hydrocarbons are higher auxiliary hydrocarbon injection pressures (3 MPa), but with shorter durations and longer intervals (3 s) between injections. Hydrocarbons with eight to ten carbons were shown to be preferred. Better mixing allowed the goals of >75% NO_x reduction with <2% fuel penalty to be achieved at critical HT operating points, including peak load at intermediate engine speeds. Bisaiji *et al.*[32] improved the performance of the system wherein hydrocarbons are dosed into the LNT at a variable lean level on a 1–2.5 Hz frequency.[30] Catalyst improvements increase efficiency 2.3×, while better hydrocarbon control increases the utility of the hydrocarbon.

Zheng *et al.*[33] show the above concept can also be used to extend the low-temperature regime if the NTC is layered underneath an SCR catalyst. At a space velocity of 80 000 h^{-1} the deNO_x efficiency of a NSC is increased from

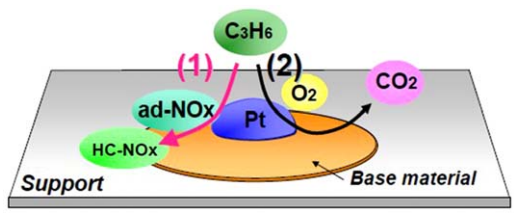

Figure 1.6 Schematic of the reaction mechanisms providing HT NO_x reduction by operating an NTC under relatively high frequency air : fuel ratio oscillations.
Reprinted from A Study of the NO_x Reduction Mechanism for Improving the Performance of Di-Air, K. Yoshida, Y. Bisaiji, N. Takagi, M. Inoue, K. Umemoto and T. Fukuma, 4th IAV MinNO_x Conference, 12–13 June 2012, Berlin.

30% to 55% using the layering approach. It is thought the SCR layer holds HC intermediaries which aid in the NO_x reduction process.

NTCs can be managed in different ways to get better high-load or transient efficiencies. Yasui *et al.*[34] run either rich and/or stoichiometric during transients depending on conditions, and use the three-way catalyst functionality of the NTC to reduce NO_x during these periods. System cycle-averaged efficiency increases from 65% to 80%, and the fuel penalty drops from 5% to 4.5%.

1.3.3 NTC + SCR Combination Systems

The most promising approach to implementing NTCs much more broadly is to couple them with a ''passive'' SCR (no urea system) or as a LT supplement to a urea-SCR system. In the non-urea approach, the NTC does most of the NO_x reductions and the SCR catalyst traps and utilizes the ammonia that is generated in the NTC during the rich regeneration phase, to supplement lean deNO$_x$. Grubert *et al.*[35] added SCR catalyst to the DPF (SCR filter) in an NTC system and improved NO_x removal efficiency by 8–20%, depending on test cycle. The NSC removes 55–70% of the NO_x, depending on cycle, and the passive SCR removes 3–20%. Both NSC NH_3 generation and SCR efficiency are dependent on temperature. Kreuz *et al.*[36] presented results using only the NH_3 coming from the NSC – the ''passive'' SCR system reduces NO_x nearly 80% on the WLTC with only 7% reductions coming from the SCR unit. On the cold start portion of a city cycle all the NO_x reduction is done by the NTC. Storms *et al.*[37] evaluated the best rich operating parameters for maximizing NH_3 generation from the NTC. At 370 °C using engine exhaust, richer conditions give higher selectivity to NH_3 (*vs.* nitrogen) from the NO_x reduction. They chose $\lambda = 0.92$ as the best for their work. Increasing the stored NO_x increases the peak NH_3 generation after the oxygen is consumed at the beginning of the rich cycle. Because of this early peak in NH_3 generation, more NH_3 is produced from multiple short rich periods than from one long one. Assuming all the NH_3 is utilized in the downstream SCR, one can achieve 5% additional NO_x removal per 1 g-CO_2 km^{-1} increase.

Kreuz *et al.*[36] also looked at urea-SCR filter in combination with the NTC. Figure 1.7 shows the explored systems and some results. In WLTC testing the SCR filter removes 42% more NO_x than a separate and larger (27%) SCR unit behind the filter. Others have attributed this to more rapid heat-up of the SCR in the filter position. An auxiliary SCR catalyst added after the SCR filter removes no NO_x on the WLTC, but adds about 10% deNO$_x$ efficiency on a highway cycle. On warm start and highway cycles, it matters little on absolute NO_x removed whether the SCR volume is distributed between a filter and downstream substrates. Seo *et al.*[38] reported on an NTC ammonia SCR filter system with an auxiliary SCR catalyst, similar in design to the one Kreuz *et al.* described. In their system 80% of the WLTC NO_x was reduced by the NTC on the WLTC (*vs.* 50–55% for Kreuz *et al.*). The downstream SCR units removed similar percentages of the NO_x to those achieved

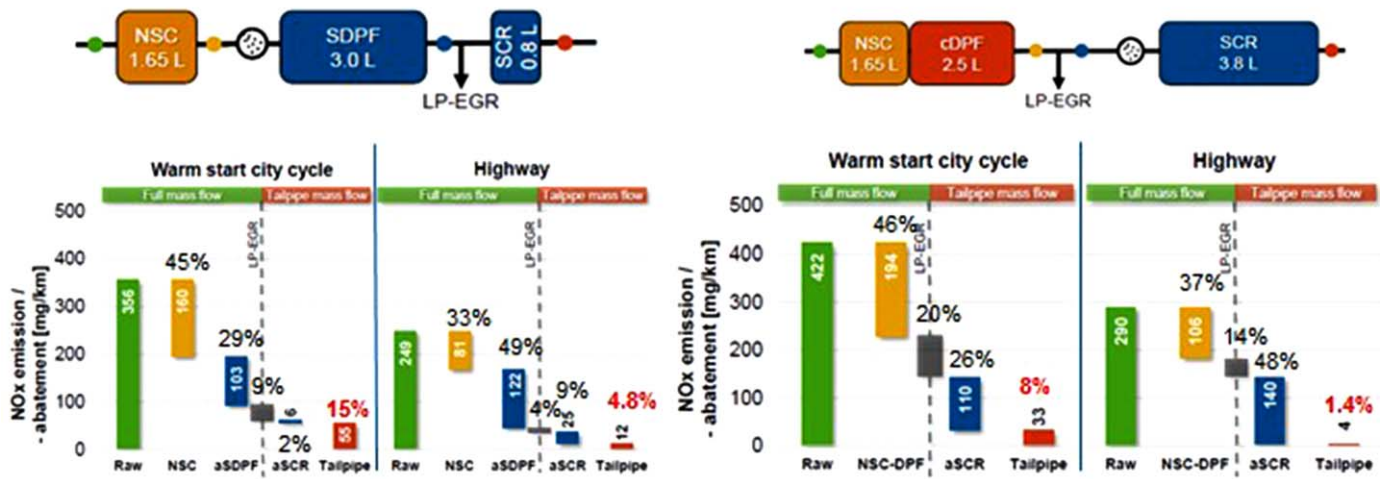

Figure 1.7 The deNO$_x$ efficiency of various components under different driving conditions for two different NTC (NSC here) + SCR combinations.
Reprinted from Challenge to Euro-6c Using Accurate Engine Management Control, G. Grubert, A. Punke, M. Hilgendorff, T. Neubauer, M. Caudle and Y. Li, 5th MinNO$_x$ Conference, June 25–26, 2014, Berlin, Germany.

by Kreuz *et al.* In this design, wherein more NO_x reduction is shifted to the NTC, yet active SCR is available for high-load driving, urea consumption and tailpipe NO_x emissions are both very low. When a DOC is replaced with an NTC in a urea-SCR system, the NO_x emission is cut more than 50% on the NEDC (New European Drive Cycle) due to better system low-temperature performance.[39] Conversely,[40] keeping the deNO_x efficiency the same, adding an NTC to a urea SCR system increases the fuel penalty by 0.4–0.6%, but drops urea consumption by 40–50%.

Interestingly, Euro 6 OBD (on-board diagnostics) for these NTC + SCR systems can be straightforward as each deNO_x component can remove enough NO_x to keep the tailpipe level below the OBD threshold.[41] The threshold is crossed only if both components malfunction.

One might consider adding some LNT to the DPF, similar to the DPNR (diesel particulate and NO_x reduction) catalyst Toyota introduced more than 15 years ago. However, Matarrese *et al.*[42] found that the presence of soot decreases the NO_x storage capacity of the LNT about 10–30% due to the competition for NO_2 between the soot and the NO_x storage sites. Soot also decreases the stability of the stored NO_x, and there are indications of oxidation of soot by the stored nitrates. Further, soot combustion caused the Pt–K/Al_2O_3 catalyst to age, resulting in 40% less NO_x storage capacity and lower soot oxidation activity.

1.3.3.1 Passive NO_x Adsorbers (PNA)

As in a NTC in which NO_x is released by dissociating the nitrate using rich gas mixture, PNAs function by thermally releasing the NO_x. For US light-duty diesels and for the emerging California HD low-NO_x technology assessment, removing cold start NO_x emissions is key to meeting the tailpipe emissions regulations. A new combination NO_x adsorber and SCR catalyst configuration was shown by Henry *et al.*[43] The system consists of an upstream passive NO_x adsorber (PNA) that might capture 65% of the NO_x at temperatures less than 150 °C, and then passively release it at temperatures greater the 150 °C. At these temperatures a copper zeolite is just becoming active and can reduce some of this released NO_x. The technology enables NO_x reductions of about 15 mg mile^{-1} (24 mg km^{-1}) on the US LD test cycle. Walker[44] reported on improvements in prototype PNAs wherein 90% of the NO_x is adsorbed at 80 °C, and held up to 250–300 °C, well within the range of SCR catalyst activity. Wylie[45] reported that on the NEDC about 10% of the engine NO_x was removed by the NO_x adsorber and converted in the SCR. NO_x emissions are 25% lower than if a DOC is used instead of the NO_x adsorber.

Regarding improvements in composition, Harle *et al.*[46] showed PNA improvements by modifying the ceria component with basicity adjustment. The ceria shows high lean NO_x removal efficiency (~60–70%) at 120 °C for NO compared to baria (45%). This is important because little NO_2 is formed at that temperature. The NO_x is released in lean conditions first at 220 °C and more at 335–350 °C depending on formulation. This feature makes the PNA

an attractive candidate for use ahead of an SCR catalyst to enable a wider range of NO_x control. Theis[47] further characterized the performance of PNAs that release NO_x at lower temperatures. Storing NO_x as a nitrate is preferred, as it releases the NO_x at a somewhat higher temperature, and is more sulfur tolerant. Theis also shows NO_x is released at higher temperature in the presence of hydrocarbon (C_2H_4). Chen[48] evaluated different Pd-zeolite structures, BEA, MFI, and CHA, and compared the performance to ceria-based adsorbers. Palladium at the exchange sites adsorbs NO directly as nitrate, other non-zeolite supported Pd catalysts need availability or formation of nitrates for significant storage. They each have different adsorption temperature curves, with the BEA capacity decreasing with temperature from 80 to 170 °C, the MFI increasing with adsorption temperature to 100 °C then gradually decreasing, the CHA rapidly increasing to 100 °C and remaining constant or increasing, while ceria is relatively constant from 80 to 170 °C. The BEA has the highest NO_x storage capacity (+50% *versus* ceria), followed by MFI, and then CHA. All the zeolites show significantly better sulfur tolerance than ceria. Desorption temperature followed capacity, with BEA starting at 200 °C and peaking at 250 °C, MFI starting at ~220 °C and peaking at 280 °C, and CHA starting at 250 °C and peaking at 370 °C. Walker[49] showed how advancements in the understanding of these materials can translate into improved system performance. Second-generation adsorber material holds more than 2× the NO_x at 130 °C *versus* the first generation, and releases it at 60 °C higher temperature (240 °C). A downstream SCR (on DPF) captures most of the released NO_x.

1.3.4 Diesel Particulate Filters

Diesel particulate filters (DPFs) have been used commercially in the LD sector since 1999, and since 2007 in the HD sector. By 2020, new diesel vehicles in all major markets (excluding South America) will require DPFs.

Heibel[50] updated the state of HD DPFs with regard to soot regeneration methods and ash impacts. Engines that have $NO_x/PM > 200$ usually have very little soot accumulation on the filter, as NO_2 oxidation of the soot "passively" occurs. Occasionally (20 000 km) an active measure is needed to clean or baseline the filter. The temperature is increased to 450 °C for up to perhaps 30 min. For engines calibrated at lower $NO_x/PM \approx 75$, soot accumulates on the filter and active regeneration every 3000–3500 km at 525–550 °C occurs for about 20–30 min to fully clean the filter. Heibel also sees "line of sight" to full useful life ash capacity, citing progress in DPF design. "Baseline" filters can store ~900 g ash and need cleaning at about 500 000 km. Emerging filters that are 15% smaller can store 1700 g of ash possibly going more than 900 000 km without cleaning.

Li *et al.*[51] studied the oxidation of soot by NO_2 in the filter. They observed that soot within the porosity oxidized first, quickly dropping back pressure. In the next regime, soot was mainly burned at the soot–wall interface. The source of this NO_2 is the oxidation of NO on the catalyst residing in the filter

wall near the soot interface, and the back-diffusion of this NO_2 to the soot. On average, the NO is recycled five times in the beginning of the soot burn and three times after an hour at 400 °C. The recycling and soot burn rates decrease due to the increasing gap between the soot and catalyst sites. Aging of filter can lead to highly variable NO_2 production rates, but pre-calcining of the washcoat at 700–800 °C stabilizes the NO_2 production. The Pt : Pd ratio also impacts NO_2 generation stability.

When SCR catalyst is added to the DPF, it consumes the NO_2 that would otherwise recycle within the Pt-catalyzed filter, greatly impairing the NO_2 ''passive'' regeneration of the soot. If active high-temperature soot regeneration is needed on SCR filters, Cumaranatunge[52] observed that, even though the high-temperature regeneration is done by burning soot with oxygen, it takes longer: 30 min at 600 °C to burn 80% of the soot on a SCR filter *versus* 10 min for normal Pt-catalyzed soot filters (CSF). Urea injection during regeneration made little difference, but NO concentration did. Even though NO_2 make is low (~10%) over the platinum in a CSF, it enhances the soot burn significantly due to an internal NO–NO_2 recycling effect between the soot and the catalyst. For an SCR filter, the only NO_2 comes from the DOC, and although it drops from 2% inlet to 0.3% outlet in the SCR filter, this is minimal. In a CSF the NO_2 increases from 2% to 7%.

Walker[53] used SCR coating design and location on the DPF to reduce this negative soot regeneration impact of SCR filters without impairing deNO$_x$ performance or back pressure. There was very little soot build on the new SCR filter over 90 US FTP (Federal Test Procedure; the US HD transient test) cycles. In addition, ash accumulation in the SCR filters has no discernible impact on NO$_x$ reduction efficiency, and the ash can be cleaned off, restoring original back pressure and performance.

1.3.5 Gasoline Emission Control

Gasoline powers the vast majority of automobiles in the world. Only Europe and India have near-equal splits between new diesel and gasoline cars. As such, gasoline emissions are the majority of mobile source toxins. Gasoline engines emit multiples higher NO$_x$ than diesel engines, but because they are stoichiometric the modern three-way catalysts (TWCs) reduce the NO$_x$ by >99%.

TWCs make use of slight rich-lean modulations (~1 Hz) and the property of the TWC to have high deNO$_x$ efficiency over rhodium, and to a lesser extent, palladium catalyst on the rich side, and high hydrocarbon and CO oxidation efficiency in the slightly lean conditions. Closed-looped control using oxygen sensors in the exhaust is key to proper air–fuel control for highly efficient TWC function. Also critical is the use of oxygen storage catalyst (OSC), like ceria, as a washcoat on which the precious metal is supported. It traps oxygen in lean conditions and uses it in the rich mode to maintain oxidation reactions during rich periods.

However, lean-burn gasoline engines are emerging for lower CO_2 emissions. NO_x from these engines is generally too high to make urea-SCR practical. Consequently, combinations of TWC, NTC, and passive-SCR are being explored.

Further, given that DPFs essentially drive LD diesel fine particle emissions down to ambient levels (or below), the particulate emissions from gasoline engines, especially direct injection engines, are relatively high and a focus of health experts and regulators. Gasoline particulate filters (GPFs) are now emerging to address this.

1.3.5.1 *Three-Way Catalysts (TWC)*

Since the mid-1990s, when the TWC was perhaps in its third generation, emissions have dropped more than 95% and PGM loading is down perhaps 70% of what it was then. Progress is still continuing.

For example, Aoki *et al.*[54] reported on complex TWC coating architectures as a way of improving performance and reducing precious metal loadings. They showed that HC light-off time is reduced 50% if all the palladium is concentrated in the front 20% of the catalyst substrate, Figure 1.8. Conversely, because rhodium is poisoned by phosphorous poisoning (from lube oil ash), it should be concentrated in the back 20% of the substrate. They also showed that ceria-zirconia washcoats can be formulated for different properties and distributed on the substrate accordingly. Zirconia-rich recipes (0–0.40 ceria : zirconia mole ratio) release oxygen fastest, and therefore should be in the front half of the catalyst, while ceria-rich formulations (0.8–1.2) store more oxygen, and are best located in the back half. To wrap up the study, the authors showed that an alumina addition can prevent zirconia

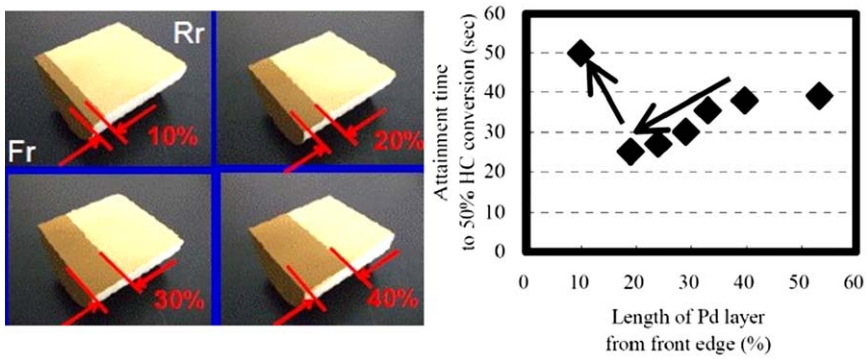

Figure 1.8 Preferentially "zone coating" Pd catalyst in the front of the TWC helps reduce the time to oxidize hydrocarbons.
Republished with permission of SAE International, from Development of Advanced Zone-Coated Three-Way Catalysts, Y. Aoki, S. Sakagami, M. Kawai, N. Takahashi, T. Tanabe and T. Sunada, *SAE Technical Paper*, 2011, 2011-01-0296, Copyright © 2011.

sintering and allow better rhodium dispersion, and niobia can prevent grain growth of rhodium catalyst.

Matsuzono *et al.*[55] describe a layered catalyst for improving performance of both close-coupled (placed on the exhaust manifold outlet) and underbody catalysts. The improvements cut PGM (platinum group metal) usage by 75% while meeting the new California LEVIII SULEV30 standard (Low Emission Vehicle III, Super Ultralow Emission Vehicle – 30 mg mile^{-1} non-methane HC + NO$_x$). The close-coupled catalyst is layered with higher-activity palladium and lower oxygen storage catalysts (OSCs) on the top, to better withstand phosphorous poisoning and to achieve better HC conversion. The catalyst demonstrates that Pd-only catalysts can have application for the lowest emissions applications. The underbody catalyst utilizes zirconia-based OSC, allowing 50% less rhodium to be used *versus* the current version of catalyst.

Hashimoto *et al.*[56] demonstrated the effectiveness of Ba/Zn/CeO$_2$ as a support alternative to Al$_2$O$_3$ for improved emissions conversion. The Al$_2$O$_3$ from the Pd/Al$_2$O$_3$/OSC formulation in the first layer of an underfloor catalyst was replaced with Ba/Zn/CeO$_2$, and this led to a 10% reduction in NMOG + NO$_x$ emissions over the LA4 test cycle using a 2011 Civic (PZEV, 1.8L L4). The Zn reduced the oxygen binding energy, increasing the O-availability and CO oxidation at low temperatures, while the barium reduces CO$_2$ adsorption which limits the oxygen availability. The principle and some results are shown in Figure 1.9. This catalyst was commercialized and applied to the 2016 Honda Civic.

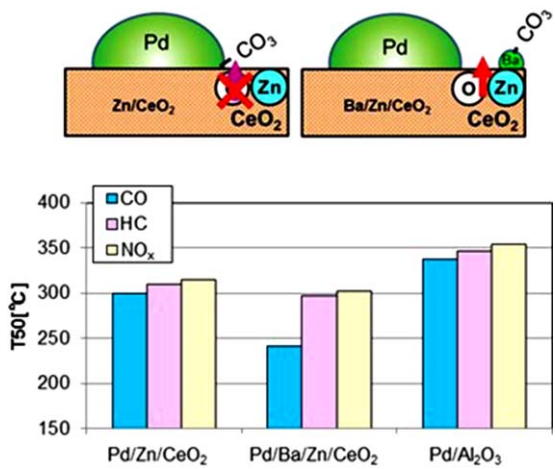

Figure 1.9 Zinc and baria additions to TWC washcoat drops the temperature for 50% conversion of CO, hydrocarbon (HC), and NO$_x$.
Republished with permission of SAE International, from Development of Low Temperature Active Material for Three Way Catalyst, M. Hashimoto, Y. Nakanishi, H. Koyama, S. Inose, H. Takeori, T. Watanabe, T. Narishige, T. Okayama and Y. Suehiro, *SAE Technical Paper*, 2016, 2016-01-0932, Copyright © 2016.

Miura *et al.*[57] investigated multiple methods of improving TWC performance. To balance the adverse effects of oxidative interaction between rhodium and the oxygen storage catalyst (OSC), yet to take advantage of the inhibition of catalyst sintering offered by the OSC, they optimized the formation of rhodium clusters on the OSC. They also developed an improved ceria-zirconia OSC with higher oxygen capacity but slower kinetics that can be axially zoned to improve system response to lean fluctuations when NO_x emissions are observed. The improvements halve the PGM loadings without compromising emissions performance.

To heat up the catalyst faster, Otsuka *et al.*[58] reported on a new substrate material with 30% less mass that provides faster heat-up and reduced emissions (Figure 1.10). FTP-75 NMOG (non-methane organic gases) and NO_x emissions are reduced by about 10% as a result. The researchers show lower temperatures on decelerations for the new material, but this has no impact on emissions. The researchers expect the developed catalyst to perform even better as the exhaust temperatures decrease as engine efficiency improves.

Another approach to reducing cold start emissions was described by Murata, *et al.*[59] The use of zeolites to adsorb cold start hydrocarbons has been investigated for many years. However, these investigators found that when palladium is added to a ZSM-5 zeolite, NO_x can be stored at 50 °C and released at 200 °C. The zeolite also adsorbs hydrocarbons. In a vehicle test, the HC and NO_x desorption temperatures are close to each other so it is thought the released HCs help in NO_x reduction. Cold start NO_x emissions are reduced about 75%.

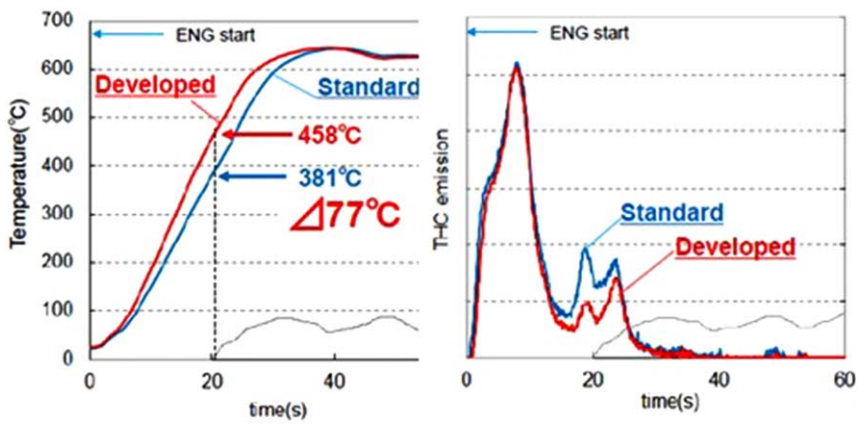

Figure 1.10 A new TWC substrate with 30% less mass heats up faster for reduced hydrocarbon emission during the FTP-75 cold start idling period (0–20 s). Republished with permission of SAE International, from Development of a Super-Light Substrate for LEV III/Tier3 Emission Regulation, S. Otsuka, Y. Suehiro, T. Tanner, D. Bronfenbrenner, T. Tao and K. Twiggs, *SAE Technical Paper*, 2015, 2015-01-1001, Copyright © 2015.

N_2O is a powerful greenhouse gas and will become increasingly more important as part of the emission inventory of gasoline engines as the CO_2 emissions drop further. Ball *et al.*[60] examined the N_2O emissions from vehicles certified to California's SULEV (Super Ultra-Low Emission Vehicle) level. Three-way catalysts produce more N_2O emissions with aging. Three cars aged for 6400 km produced < 1 mg mile^{-1} N_2O during the FTP; all of the vehicles with dynamometer aged catalysts produced between 1.2 and 8 mg mile^{-1} of N_2O, which is below the 10 mg mile^{-1} regulation. This represents perhaps 0.2–1.5% of the GHG footprint of emerging vehicles (2020 in Europe). More severely aged catalyst may exceed the 10 mg mile^{-1} N_2O US LD GHG limit. There appears to be many system interactions (calibration, fuel injection, catalysts and their combinations, *etc.*) other than catalyst temperatures that effect N_2O emissions. In general, aged catalysts produce N_2O emissions at between 300 and 500 °C. The period after a hot start can produce much of the N_2O emissions due to extended periods of time when both the close coupled and underbody catalysts are in this temperature range. Secondary air injection does reduce cold start N_2O formation, but lowering the ceria in a close-coupled catalyst increases N_2O formation during the FTP at exhaust temperatures of 550 °C.

Catalyst durability requirements are increasing, so understanding the aging and testing for it are important. Fathali[61] showed that, for fresh and 40-hour aged samples, fuel-cut after acceleration has the highest contribution towards deactivation of the catalyst system. In addition, the retardation fuel-cut is detrimental to the catalyst system but not to the same extent as an acceleration fuel-cut. During the aging procedure, exotherms were observed at the start of fuel-cut and the intensity of these exotherms increases with the length of aging time. The increasing exotherms are explained by the decomposition of hydrocarbons into C and H_2, and their subsequent oxidation at lean conditions. In addition, fuel-cut-off temperature measurements demonstrate that the magnitude of those exotherms is related to the total number as opposed to the total length of the fuel-cut.

Emissions systems durability requirements are increasing to 150 000 miles (240 000 km) in California LEVIII and US Tier 3 emissions regulations. Fathali *et al.*[62] looked carefully at aging protocols. Mass flow during the catalyst aging plays an important role with lower mass flows deactivating the inlet of the catalyst, and conversely with increased mass flows the deactivation zone moves rearward. Catalyst exotherms when aging with poisons (like from lube oil) shift more rearward in the catalyst, as the poisons impact the active catalyst sites toward the inlet of the catalyst. Exotherms during a secondary air injection aging cycle without poisons can be modeled, which can be useful in aging studies and in predicting end-of-life emissions.

System design and calibration are significant contributors to low gasoline emissions. Ball *et al.*[63] benchmarked gasoline engine and catalyst emissions technologies on two gasoline cars certified to Tier 2 Bin 5 standards, and two certified to California PZEV (Partial Zero Emissions Vehicle) standards (similar to LEVIII fleet average) in the 1.4–2.0 liter engine class. The Bin

5 cars had specific power ratings of 88 and 100 $kW\,L^{-1}$, and the PZEV cars were 12% lower at 77–83 $kW\,L^{-1}$. Common technologies among the four engines are variable valve technologies (to various degrees), and single stage turbocharging with a close-coupled catalyst. Both PZEV cars used wide range oxygen sensors and underbody catalysts. The authors looked at idling speed, air–fuel ratio, and ignition timing to quickly heat the catalyst. The PZEV engines idle slower (900 and 1300 RPM *versus* 1500 RMP), deliver lean mixtures ($\lambda = 1.05$) to the catalyst (one Bin 5 is rich, the other lean), and both retard spark until 20 °C after top center (*versus* 10 °C for the Bin 5 cars) to delay the fuel burn for hotter exhaust. These measures allow the catalyst on PZEV cars to reach 300 °C within 10 s during idle, while the Bin 5 cars take 20–30 s, into the first hill, on the US FTP. It was demonstrated that through proper catalyst design and placement of the precious metals, significant reductions in precious metal loading are possible with minimal impact on exhaust emissions. For example, nearly 4 g of Pd was taken from the underbody catalyst in one design while still meeting the Bin 5 emissions regulations. In addition, significant interactions between catalyst technology and lambda control exist, especially with deceleration fuel cut-offs (DFCOs). For example, higher oxygen storage capacity can drop NO_x emissions upon acceleration after a DFCO event. New technologies like HC traps can reduce emissions by about 15% in the early portions of the US FTP, but upwards of 30% when DFCOs are used. These examples show that gasoline emissions systems need to be designed much more closely with the engine calibration as the greenhouse gas and criteria emissions tighten.

Finally, on-board diagnostics (OBDs) are central to reducing in-use emissions and are getting more demanding. The state of oxygen storage in a TWC, as indicated by oxygen sensors before and after a catalyst, is one of the main indicators of a well-functioning TWC. Moos[64] summarizes the application of a radio-frequency method for helping to develop these algorithms or for direct on-board measuring of the oxygen stored in the TWC. Advantages include measuring the state of the catalyst directly as a function of time, rather than seeing a step change in oxygen sensor signal at $\lambda = 1$; and being better-able to determine the CO–NO_x cross-over point if different hydrocarbons are dominating, for example with flex-fuel vehicles.

1.3.5.2 Gasoline Particulate Filters

Because ultra-fine particle emissions are toxic,[65] and can arise from high gasoline direct injection engines (GDI), they fall under a particle number (PN) regulation in Europe, China, and India. The limit value for GDI PN emissions will be the same as for light-duty diesel cars in 2017 (Euro 6c). However, contrary to the case for diesel, the limit value in certification testing can be met by either engine means or with gasoline particulate filters. Still, and because they are relatively new and just emerging commercially, gasoline particulate filters (GPFs) are the leading topic now in vehicular emission control.

1.3.5.2.1 Nature of Gasoline-Derived PN. Lee *et al.*[66] investigated the nature of GDI soot. Crystalline structures of GDI soot are slightly less ordered than those of diesel soot, except for the idling condition, and do not change significantly with engine operating conditions. Examination of the sub-23 nm particles in a high-resolution transmission electron microscope shows clear carbon fringe patterns, confirming these particles are carbonaceous; but they have a lower degree of crystallinity than the smaller diesel particles.[67] Maier *et al.*[68] tentatively conclude that sub-10 nm particles do not, for the most part, originate from the combustion of the fuel, but likely come from the lube oil. Czerwinski *et al.*[69] found the sub-30 nm particles have the highest concentration of lube oil ash components, with calcium being an order of magnitude higher in concentration than other metals, while the larger size fractions contain metal oxide particles from wear components.

Fuel composition and properties naturally affect the combustion characteristics and resulting particulates. Addition of components with higher resistance to volatilization or increased propensity to form soot precursors (*e.g.* aromatics) lead to increased particulates. On the other hand, components such as ethanol which add oxygen or those that improve volatility can be expected to lower particulates.[70,71] However, ethanol can have mixed effects on particulates and also depends on the blending method, with splash blending leading to a decrease in PN while match blending leads to an increase in PN.[72]

More studies are emerging quantifying the impact of fuel injector deposits on increasing particulates. Wen *et al.*[73] examined the morphology of injector deposits and their impact on spray pattern and ultimately the emissions, from a 1.6L naturally aspirated GDI engine certified to China 5. Comparing coked and rinsed injectors, the authors found an increase in particulate mass emissions with coked injectors that were 4.76× that of clean injectors.

Cold starts have high particulate emissions due to lower fuel volatility, fuel impingement on colder surfaces, and less time for evaporation. Cold ambient temperatures can have a similar effect. H. Badshah *et al.*[74] studied the particle emissions from 11 PFI (including a hybrid), 10 GDI and 2 diesel vehicles with DPFs under cold-cold start (sub-zero temperature) conditions. When tested over the NEDC test cycle, almost all gasoline vehicles (including PFI) exceeded the EU regulated PN limit of 6×10^{11} # km^{-1}. Interestingly, the average PN during the initial 180 s was almost identical for both GDI and PFI vehicles (although particles in PFI were much smaller and under the 23 nm cut-off).

Besides cold start, other operating conditions also affect PN emissions. Schmitz *et al.*[75] show that, although a Euro 6a car might meet the PN standard on certification test cycles without a GPF, under a high-speed test cycle (RTS95) the PN emissions are more than 3× higher than measured on the WLTC, and more than 2× the limit value. Seong[76] shows that GDI PM and PN emissions markedly increase if the cooling water temperature is 40 °C or lower, wherein cold transients emit 10–15× more PN than hot transients, which emit 4–5× more than steady state operation.

The association of increased polycyclic aromatic hydrocarbon (PAH) emissions from GDI engines is becoming known.[77,78] This most likely follows from the role of PAH precursors in the formation of soot.[79] Karavalakis *et al.*[80] showed a 2014 GDI pick-up has 14× more total PM-bound PAH emissions than a similarly powered PFI truck, and ~4× more gas-phase PAH emissions. There is evidence that the PAHs are likely adsorbed on soot and removed using GPFs. Karavalakis found two- and three-ring PAHs emissions from 2 GDI vehicles and heavier carcinogenic compounds from one of the vehicles tested. Vapor phase PAHs were very high (0.1 mg mile^{-1}), while these reduced by 50% with the use of GPFs.

There are new studies which look at their impact of some new engine strategies on particulates. Storey *et al.* examined the impact of start–stop technology.[81] Particulate emissions were characterized from a GDI vehicle using fuels splash-blended with ethanol (20%) and iso-butanol (12%), with and without start–stop operation. Their study showed that start–stop leads to similar or lower particulate mass and number, and that E20 fuel led to lowest PM as well as PAHs. However, S. Zinola *et al.*[82] operated a GDI engine on an engine bench, simulating HEV operation by stopping and starting the engine during NEDC testing. Although the engine only operated 28% of the time during the cycle, the PN emissions were 4.5× higher than when the engine was run in conventional mode. More work is needed, but as stop–start and hybrid systems propagate this could become an exposure issue at major intersections and even during normal HEV operation.

Due to all these variables, fuel quality, ambient temperature, deposit formation, and toxic PAH emissions, combined with regulatory scrutiny and RDE regulations out to full useful time, GPF interest is very high.

1.3.5.2.2 GPF PN Filtration Efficiency and Performance. GPF performance is improving and several studies have demonstrated the ability of GPFs to reduce tailpipe particulates below the regulations and over the vehicle lifetime.

Work by Chan *et al.*[83] was reported on the importance of pre-conditioning on filtration efficiency. They measure 80+% filtration efficiency on US FTP-75 cycle with a clean uncoated filter, but upwards of 95+% efficiency after 230 s of operation. Conversely, as shown Figure 1.11, on the much-hotter US06 cycle, the filtration efficiency has no temporal relationship because it would periodically regenerate throughout the cycle. Note the high filtration efficiency in the smaller size fraction (< ~20 nm) due to Brownian movement of the particle, and in the larger size fraction >250 nm due to interception mechanisms.

Black carbon is emerging as a potent greenhouse gas, even though it is short-lived, as it might be 2000× more potent than CO_2. The UN International Panel on Climate Change reported black carbon is the second highest contributor to anthropogenic climate change.[84] Chan *et al.*[85] found that GDI vehicles (model years 2011 and 2012) have black carbon emissions on the order of 1.8 mg km^{-1} as measured on the high-load US06 test cycle and Phase 2 and 3 of the US FTP-75 test cycles. GPFs reduce these emissions

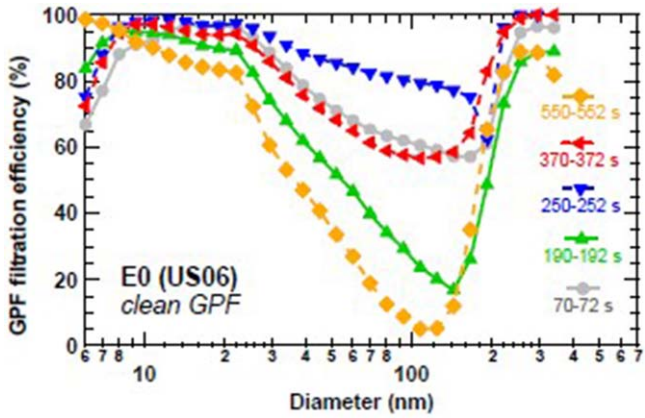

Figure 1.11 Size dependent filtration efficiency of an uncoated GPF on the US06 as a function of time. There is no temporal relationship in the mid-size range due to periodic burning of the filter cake.
Republished with permission of SAE International, from Evaluation of a Gasoline Particulate Filter to Reduce Particle Emissions from a Gasoline Direct Injection Vehicle, T. W. Chan, E. Meloche, J. Kubsh, D. Rosenblatt, R. Brezny and G. Rideout, *SAE Int. J. Fuels Lubr.*, 2012, 5(3), 1277, Copyright © 2012.

by 80% or the equivalent of 2.9 g CO_2 (eq) km^{-1}. This is about 2.4% of the average allowable CO_2 emissions in the US in 2020.

Impact of GPFs on fuel economy is a key consideration, and several studies have shown that system backpressure can be maintained relative to the base OEM system. Chan *et al.*[72] found that CO_2 emissions for GDI vehicles with and without a catalyzed GPF to be within the measurement uncertainty over the FTP-75 and US06 test cycles. In their study on the impact of ash of GPF performance, Lambert *et al.*[86] found no significant increase in fuel consumption after 130 000 miles of vehicle aging, despite the ~2× increase in pressure drop due to accumulated ash. Engine performance impacts after 160 000 km are minimal,[87] with only 2.5% loss of peak power and <1% loss of peak torque, with no deterioration in fuel consumption.

Richter *et al.*[88] evaluated two TWC-coated configurations, wherein the total PGM loading in one configuration was the same as the base design but was distributed between the close-coupled TWC and the GPF; the other configuration had an optimized coating. With the same PGM loading, the investigators found the NO_x emissions dropped 20% *versus* the baseline. With an optimized zone coating on the close-coupled catalyst, 6% less PGM was used compared to the baseline, NO_x emissions remained at the low level, but CO emissions dropped 30% from the other GPF case. Blakeman[89] described a coated GPF that can meet Euro 6 requirements by itself. Two designs are shown – one designed for low emissions and the other for low back pressure. The low emissions design has 10% lower PN and 30% lower NO_x emissions, but at a 50% higher back pressure during accelerations.

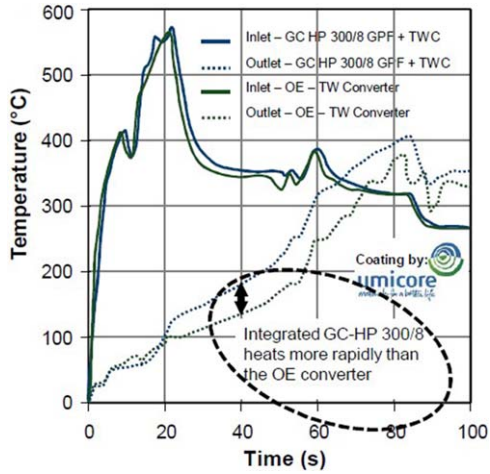

Figure 1.12 Catalyzed GPF (gasoline particulate filter) heats up faster after 20 s than the stock TWC (three-way catalyst).
Reprinted from D. Rose, T. Boger, R. Ingram-Ogunwumi, and C. Bischof, 22nd Aachen Colloquium on Automobile and Engine Technology, October 2013.

Substrates and catalyst coating methods are advancing to the point where back pressure and light-off of coated GPFs are nearly equivalent or better than production TWC. Rose *et al.*[90] found the heat-up results presented in Figure 1.12. The inlet temperatures are nearly identical in the case of the TWC and the catalyzed GPF, but after 20 s the GPF outlet temperature increases faster than those of the TWC. By 40 s the GPF is 50 °C hotter. The effect is attributed to low thermal mass and better heat transfer kinetics in the wall-flow design. In other tests, back pressure for a coated GPF is lower than for a standard TWC in low and intermediate flow conditions (-50% at 200 $m^3\,h^{-1}$) at 750 °C, but is higher at high flow conditions ($+30\%$ at 700 $m^3\,h^{-1}$).

The durability of coated GPFs was demonstrated for a 1.4L GDI engine in China.[91] After 160 000 km testing, the engine-out emissions were unchanged. The TWC performance was robust, with only a slight (~15 °C) increase in light-off temperature, and with a high filtration efficiency (~85%) maintained through the lifetime.

1.3.5.2.3 Ash Impacts. The role of ash and soot on GPF performance is being quantified. Lambert[92] showed that accumulation of low amounts of soot and ash on the filter wall can lead to a large increase in filtration efficiency. Filtration efficiency improved from ~60% under clean conditions to 90% with accumulation of 0.08 $g\,L^{-1}$ of soot and to 80% with 1 g of ash. It was also shown that high washcoat loading is not as effective for improving filtration efficiency. An ash accumulation study[93] on an under-floor GPF after 240 000 km on a 3.5L GDI vehicle showed that only 50% of ash was collected from engine oil sources, while the rest was derived from

corrosion material (20%) and from catalytic washcoat from the upstream TWC. Ash was distributed ~60% on channel walls and 40% as end plugs. Rose *et al.*[94] also tested the durability of bare GPFs and showed that two vehicles operated with different oils (2× difference in lube ash) gave improved PN performance over 100 000 km. Surprisingly, GPF back pressure was the same for both oils.

While the role of ash in increasing filtration efficiency and pressure drop is understood, ash is also shown to play a role in enhancing the reactivity of soot during oxidation.[95] Soot oxidation rates are increased by ratio of Ca (or Mg)/(P + Zn), rather than absolute Ca or Mg levels.

1.3.5.2.4 GPF Regeneration. Richter *et al.*[88] showed that a coated GPF regenerates PM much more readily than an uncoated part, and moving catalyst from a flow-through substrate onto a downstream GPF can drop emissions. Morgan[96] also showed that TWC formulations can also enhance soot burn on a GPF, dropping burn temperatures 100–200 °C relative to uncoated filters (675 °C). Fuel cut-offs on decelerations were shown to result in significant burning of soot due to both high temperatures and the presence of more oxygen.

Regarding GPF regeneration, gasoline and diesel soot have similar activation energies,[97] and so are expected to burn similarly. Nicolin *et al.*[98] simulated and measured the soot burn in an in-use vehicle test in which the filter was preloaded with a representative soot surrogate. Figure 1.13 shows

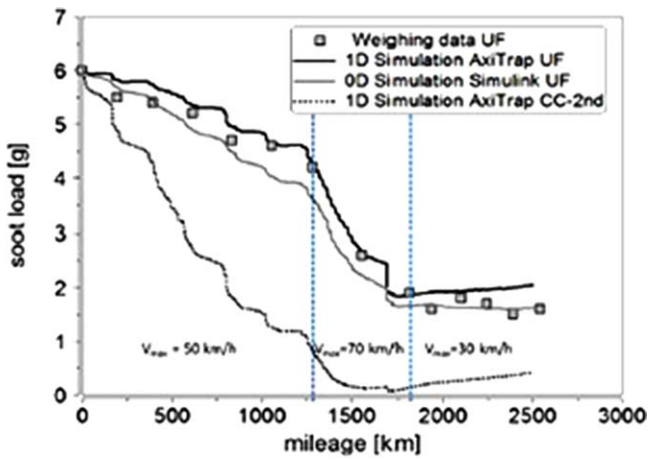

Figure 1.13 Measured and simulated burning of soot in under-floor GPFs for three different average speed regimes. Also shown is a simulation for a close-coupled GPF. Underfloor GPFs ''settle'' into about 2.3–3.0 g of soot loading, while close-couple GPFs settle to 0.6–8 g.
Republished with permission of SAE International, from Modeling of the Soot Oxidation in Gasoline Particulate Filters, P. Nicolin, D. Rose, F. Kunath and T. Boger, *SAE Int. J. Engines*, 2015, 8(3), 1253, Copyright © 2015.

the measured and simulated results for three different average speed regimes when the filter is in the under-body position. The soot is mainly burned during the lean decelerations. Only during the slow speed regime (30 km h^{-1}) was there no soot burn, but nor was there soot accumulation. Also shown in the figure is a simulated case when the filter is in the close-coupled position. Soot burn is rapid due to the higher temperatures. In low-speed driving the filter settled into 0.6–0.8 g of soot load in the close-coupled position, and 2.3–3.0 g of soot in the under-floor position, and measurements on actual filters analyzed from a range of test vehicles show similar "equilibrium loadings".

1.3.5.3 Lean Burn Gasoline

The emerging GHG emissions regulations could be addressed with lean-burn gasoline engines but, like with diesel, they have a lean-NO_x problem. However, compared to modern light duty diesel, NO_x levels during gasoline lean operation are considered too high for it to be practical to use urea-based SCR solutions.

Philipp *et al.*[99] described the emission control system for the Mercedes-Benz lean burn gasoline engine for Euro 6 and the concept system for the US version. They combine the TWC with NTC to make a single component in the close coupled position, followed by an underbody NTC. The US SULEV concept adds a TWC in front of the first NTC to deliver quicker light-off. A more significant challenge was in managing the sulfur trapped by the two NTCs. During desulfation to prevent the sulfur coming off the front NTC from depositing on the back one, two separate types of NTCs with different sulfur release properties were developed. Upon heat-up the system is designed to use a lower temperature formulation in the back than the front to match the release of sulfur at roughly the same time.

Researchers at Oak Ridge National Laboratory carried out a fundamental investigation into a TWC + SCR approach that is similar in principle to the LNT + SCR approach, wherein NH_3 is generated *in situ* by the TWC.[100] TWCs are shown to produce NH_3 over a broad temperature window. Key variables for system performance are PGM content, temperature, and control of the air : fuel ratio. Greater than 99% NO_x conversion was observed using the approach. Operating over a TWC at $\lambda = 0.96$ delivers a good balance between NH_3 generation and fuel consumption over a wide range of conditions. Adding NO_x storage material to the TWC increases lean time and decreases rich time. There is a delay in NH_3 production, however. Transient test modeling shows a 10% fuel consumption improvement using lean modes over the base GDI engine. Stoichiometric operation provides ~25% more NO_x than the lean modes, which helps to reduce the rich/lean time ratio. Prikhodko *et al.*[101] found that an excess NH_3/NO_x ratio of 1.13 at the TWC outlet is optimum for achieving 99.5% NO_x conversion, while also managing the fuel penalty and minimizing NH_3 slip. Reduced cycle time was also

found to be beneficial to reduce NH_3 oxidation during lean periods. Challenges include HC and CO slip, and sulfur tolerance.[102]

1.4 Future Perspectives

Although there is much discussion and interest in pure electric vehicles, almost all agree the internal combustion engine will continue to play a major vehicular role for decades to come. However, they will continually be under pressure to reduce criteria and greenhouse gas emissions. For example, although the California LEV3 emission levels (similar to US Tier 3) are currently the tightest in the world, California authorities are now considering another round of tightening, perhaps 60–70% to LEV4 for 2025–2030. As mentioned earlier, California is considering up to 90% further HD NO_x reductions in a similar timeframe. In addition, to meet 2040-50 GHG goals tightening of fuel consumption in the LD sector will continue at about 3–5% reductions per year, and perhaps at 1–3% per year for HD engines. Templated on top of tightening tailpipe limit values is a strong drive now towards real world emissions reductions. These can be much more demanding than those met using dynamometers. Of course, as emissions and engine efficiency targets get tighter and tighter, incremental costs for these reduction go up, sometimes rather dramatically.

Vehicle electrification through hybridization is happening now, and will continue. Hybridization generally reduces all emissions because the engine runs less and the electric motor can relieve emissions during transients and cold start. Longer term, it is reasonable that hybridization will facilitate advanced combustion strategies, like compression-ignition gasoline and various low-temperature combustion methods. All of these methods are lean, have much cooler exhausts, and higher hydrocarbon and CO emissions, but reduced NO_x emissions. However, they will need NO_x aftertreatment.

Targets for future emissions technologies are to achieve 90% emissions reductions at 150 °C on a sustainable basis (not just during start-up). Engine downsizing results in higher exhaust temperatures at high load, thus emissions control systems will need to meet a wider temperature range. NTCs are nearly if not already meeting the low-temperature requirement, but likely will need to be combined with urea-SCR to achieve reductions over the whole load range. SCR can work at the lower temperatures but, as current urea systems cannot be used at $T<180$ °C due to by-product deposits, alternative NH_3 deliver methods are needed. The trend towards combination systems and component integration will continue.

1.5 Conclusions

This chapter summarizes the state-of-the-art of emission control technologies for both diesel and gasoline engines. It covers current and emerging

regulations in the major markets; lean NO_x control using SCR (selective catalytic reduction) and NO_x trap catalysts (NTC); diesel and gasoline particulate filters; three-way catalysts (TWC); and lean gasoline NO_x control.

The USA currently has the tightest LD (light duty) and HD (heavy duty) tailpipe standards in the world for gaseous emissions. All major markets require some form of hydrocarbon and NO_x reduction technology for all vehicular engines. Europe, China, and India (in 2020) have the tightest particulate standards by virtue of PN (particle number) as the metric rather than PM (particle mass). This results in particulate filters generally being needed for all diesel vehicular engines in the major markets, for most GDI (gasoline direct injection) engines in Europe and India, and for all engines in China.

Diesel emission control technologies are covered first. SCR technology is advancing with better catalysts that have improved high-temperature durability. The various SCR catalyst types are compared with copper zeolite being the preferred family of catalysts for most applications. N_2O formation, NH_3 storage, and system control are discussed. Systems achieve nearly 100% deNO_x efficiency at high-load points, about 90 + % efficiency on LD transient cycles with cold start, and 97–98% efficiency on hot HD transient cycles. SCR catalysts are now being added to diesel particulate filters, enabling faster heat-up due to closer placement to the engine, and space savings. NTCs are improving incrementally with better low- and high-temperature conversion, sulfur tolerance, and reduced precious metal loadings. Combination NTC + SCR systems are now emerging for LD diesel applications. Passive NO_x adsorbers are described that will collect NO_x at low temperatures and release them at higher-temperatures when the downstream SCR is operative. Diesel particulate filters fall into two categories described by the soot regeneration method – low temperature (with high NO_x : soot ratio) and high-temperature (lower NO_x : soot ratio). SCR filter regeneration issues are also discussed.

The gasoline emission control discussion starts with improvements in TWC coating technology, precious metal utilization, and washcoat and substrate improvements. Gasoline particulate filters (GPFs) are new and just now starting widespread implementation in Europe and China. The nature of gasoline particulates is discussed first, followed by GPF performance, ash storage, and filter regeneration. Lean burn gasoline NO_x control uses combination TWC, NTC, and SCR systems, wherein the NH_3 for the SCR is generated in the upstream components during periodic rich excursions.

Finally, future perspectives are shared. Exhaust gas temperatures will continue to decrease as GHG reductions dominate future trends. Further criteria emissions reductions will also be needed. Advanced combustion engines utilizing gasoline compression ignition and low-temperature combustion will emerge, enabled by hybridization. Goals for all emissions control systems are 90% conversion at 150 °C.

References

1. T. Johnson and A. Joshi, *SAE Technical Paper*, 2017, 2017-01-0907, DOI: 10.4271/2017-01-0907.
2. T. Johnson, *SAE Int. J. Engines*, 2016, **9**(2), DOI: 10.4271/2016-01-0919.
3. T. Johnson, *SAE Int. J. Engines*, 2015, **8**(3), DOI: 10.4271/2015-01-0993.
4. T. Johnson, *SAE Int. J. Engines*, 2014, **7**(3), DOI: 10.4271/2014-01-1491.
5. T. Johnson, *SAE Int. J. Engines*, 2013, **6**(2), DOI: 10.4271/2013-01-0538.
6. T. G. Vlachos, P. Bonnel and M. Weiss, *36. Internationales Wiener Motorensymposium* 2015, Vienna, May 2015.
7. W. Matsui, T. Suzuki, Y. Ohta, Y. Daisho, H. Suzuki and H. Ishii, *JSAE paper* 20115720, October 2011.
8. F. Zimmermann, U. Gärtner, P. Benz, M. Ernst and J. Lehmann, Presented at *SAE Heavy Duty Emission Control Symposium 2014*, Göteborg, 17–18 September 2014.
9. M. Henry, *SAE HD Emissions Symposium*, Gothenburg, September 2016.
10. J. Girard, C. Montreuil, J. Kim, G. Cavataio and C. Lambert, *SAE Int. J. Fuels Lubr.*, 2009, **1**(1), 488, DOI: 10.4271/2008-01-1029.
11. K. Hallstrom and S. Shah, *SAE Technical Paper*, 2017, 2017-26-0120, DOI: 10.4271/2017-26-0120.
12. A. Kumar, J. Li, J. Luo, S. Joshi, A. Yezerets, K. Kamasamudram, N. Schmidt, K. Pandya, P. Kale and T. Mathuraiveeran, *SAE Technical Paper*, 2017, 2017-26-0133, DOI: 10.4271/2017-26-0133.
13. A. Kumar, M. A. Smith, K. Kamasamudrama, N. W. Currier and A. Yezerets, *Catal. Today*, 2016, **267**, 10.
14. T. Ryu, N. H. Ahn, S. Seo, J. Cho, H. Kim, D. Jo, G. T. Park, P. S. Kim, C. H. Kim, E. L. Bruce, P. A. Wright, I.-S. Nam and S. B. Hong, *Angew. Chem., Int. Ed.*, 2017, **56**, 3256, DOI: 10.1002/anie.201610547.
15. F. Gao, M. Kollár, Y. Wang, G. Muntean, J. Szányi and C. Peden, Enhanced High and Low Temperature Performance of NO_x Reduction Materials, Project ACE026, US Department of Energy Annual Merit Review, Washington, DC, June 2015.
16. Z. G. Liu, N. A. Ottinger and C. M. Cremeens, *Atmos. Environ.*, 2015, **104**, 154.
17. J. Jansson, Å. Johansson, H. Sjovall, M. Larsson, G. Smedler, C. Newman and J. Pless, *SAE Technical Paper*, 2015, 2015-01-0997, DOI: 10.4271/2015-01-0997.
18. W. Partridge, J. Pihl, X. Auvray, L. Olsson, K. Kamasamudram and A. Yezerets, *9th Catalysts for Automotive Pollution Control (CAPoC9) Conference*, September 2012, Brussels.
19. G. J. Bartley, C. J. Chadwell, T. W. Kostek and R. Zhan, *SAE Technical Paper*, 2012, 2012-01-1077, DOI: 10.4271/2012-01-1077.
20. H. Kojima, M. Fischer, H. Haga, N. Ohya, K. Nishi, T. Mito and N. Fukushi, *SAE Technical Paper,* 2015, 2015-01-0994, DOI: 10.4271/2015-01-0994.

21. Y. Yang, G. Cho and C. Rutland, *SAE Technical Paper*, 2015, 2015-01-1060, DOI: 10.4271/2015-01-1060.
22. O. Mihai, S. Tamma, M. Stenfeldt and L. Olsson, *CLEERS 2016 Conference*, Ann Arbor, MI, April 2016. See also *Ind. Eng. Chem. Res.* 2015, **54**, 11779.
23. M. Iivonen and A. Wabnig, *SAE HD Emissions Symposium*, Gothenburg, September 2016.
24. P. Chavannavar, *CLEERS 2014 Conference*, Dearborn, MI, April 2014.
25. D. Tomazic and H. Nanjundaswamy, *4th International CTI Conference on NO_x Reduction – Current and Future Solutions for On- and Off-Road Applications*, Detroit, June 2012.
26. K. Suga, T. Naito, Y. Hanaki, M. Nakamura, K. Shiratori, Y. Hiramoto and Y. Tanaka, *SAE Technical Paper*, 2012, 2012-01-1246.
27. T. Umeno, M. Hanzawa, Y. Hayashi and M. Hori, *SAE Technical Paper*, 2014, 2014-01-1526, DOI: 10.4271/2014-01-1526.
28. J. Li, N. Currier, A. Yezerets, H.-Y. Chen, H. Hess and S. Mulla, *SAE Int. J. Engines*, 2016, **9**(3), 1615.
29. Y. Bisaiji, K. Yoshida, M. Inoue, K. Umemoto and T. Fukuma, *SAE Technical Paper*, 2011, 2011-01-2089, JSAE paper 20119272.
30. M. Inoue, Y. Bisaiji, K. Yoshida, N. Takagi and T. Fukuma, *9th Catalysts for Automotive Pollution Control (CAPoC9) Conference*, September 2012, Brussels.
31. K. Yoshida, Y. Bisaiji, N. Takagi, M. Inoue, K. Umemoto and T. Fukuma, *4th IAV MinNO_x Conference*, 12–13 June 2012, Berlin.
32. Y. Bisaiji, K. Yoshida, K. Umemoto, Y. Haba and T. Fukuma, *5th MinNO_x Conference*, June 25–26, 2014, Berlin, Germany.
33. Y. Zheng, M. Li, M. Harold and D. Luss, *SAE Int. J. Engines*, 2015, **8**(3), 1117.
34. Y. Yasui, H. Matsunaga, H. Hardam, M. Yanada, T. Takahashi, M. Yamada, H. Hardam and J. Balland, *5th MinNO_x Conference*, June 25–26, 2014, Berlin, Germany.
35. G. Grubert, A. Punke, M. Hilgendorff, T. Neubauer, M. Caudle and Y. Li, *5th MinNO_x Conference*, June 25–26, 2014, Berlin, Germany.
36. J. Kreuz, H.-D. Noack, F. Welsch, J. Baron and S. Bremm, *Hyundai Kia International Power Train Conference 2015*, Korea, October 27–28, 2015.
37. W. Storms, A. Rateau, H. Matsubara, F.-A. Lafossas and A. Mohammadi, *10th Catalysts for Automotive Pollution Control (CAPoC10) Conference*, Brussels, October 2015.
38. T. M. Seo *et* al., A Development of the Combining System with LNT and SDPF for Stringent EU Emission Limits in Diesel Passenger Car, *Aachen Colloquium*, October 2015.
39. J. Wylie, D. Bergeal, D. Hatcher and P. Phillips, *5th MinNO_x Conference*, June 25–26, 2014, Berlin, Germany.
40. B. Holderbaum, *Hyundai Kia International Powertrain Conference 2014*, Namyang, Korea, October 28–29, 2014.

41. J. Köpf, A. Keber and H.-J. Brüne, *5th IAV MinNO$_x$ Conference*, June 25–26, 2014, Berlin.
42. R. Matarrese, L. Castoldi, N. Artioli, E. Finocchio, G. Busca and L. Lietti, *Appl. Catal., B*, 2014, **144**, 783.
43. C. Henry, A. Gupta, N. Currier, M. Ruth, H. Hess, M. Naseri, L. Cumaranatunge and D. Chen, *US Department of Energy Directions in Engine Efficiency and Emissions Research (DEER)*, Dearborn, MI, October 2012.
44. A. Walker, Current and Future Trends in Catalyst-Based Emission Control System Design, *SAE Heavy-Duty Diesel Emission Control Symposium*, September 2012, Gothenburg.
45. J. Wylie, *Hyundai Kia International Power Train Conference* 2015, Korea, October 27–28, 2015.
46. V. Harle, F. Ocampo, N. Ohtake and R. Rohe, *5th MinNO$_x$ Conference*, June 25–26, 2014, Berlin, Germany.
47. J. Theis and C. Lambert, *8th International Conference on Environmental Catalysis*, August 24–27, 2014, Ashville, NC.
48. H.-Y. Chen, *CLEERS 2016 Conference*, Ann Arbor, MI, April 2016.
49. A. Walker, Future Challenges and Incoming Solutions in the Global Catalyst-Based Emission Control Area, *SAE HD Emissions Control Symposium*, Gothenburg, September 2014.
50. A. Heibel, *13th Forum SAE Brasil de Tecnologia de Motores Diesel*, August 2016.
51. Y. Li, M. Weinstein and S. Roth, *8th International Conference on Environmental Catalysis*, August 24–27, 2014, Asheville, NC, USA.
52. L. Cumaranatunge, *CLEERS2016 Conference*, Ann Arbor, April 2016.
53. A. Walker, Catalyst-Based Emission Control Solutions for the Global HDD Market – What Does the Future Hold, *SAE HD Emissions Symposium*, Gothenburg, September 2016.
54. Y. Aoki, S. Sakagami, M. Kawai, N. Takahashi, T. Tanabe, and T. Sunada, *SAE Technical Paper*, 2011, 2011-01-0296.
55. Y. Matsuzono, K. Kuroki, T. Nishi, N. Suzuki, T. Yamada, T. Hirota and G. Zhang, *SAE Technical Paper*, 2012, 2012-01-1242.
56. M. Hashimoto, Y. Nakanishi, H. Koyama, S. Inose, H. Takeori, T. Watanabe, T. Narishige, T. Okayama and Y. Suehiro, *SAE Technical Paper*, 2016, 2016-01-0932.
57. M. Miura, Y. Aoki, N. Kabashima, T. Fujiwara, T. Tanabe, A. Morikawa, H. Ori, H. Nihashi and S. Matsui, *SAE Technical Paper*, 2015, 2015-01-1005, DOI: 10.4271/2015-01-1005.
58. S. Otsuka, Y. Suehiro, T. Tanner, D. Bronfenbrenner, T. Tao and K. Twiggs, *SAE Technical Paper*, 2015, 2015-01-1001, DOI: 10.4271/2015-01-1001.
59. Y. Murata, T. Morita, K. Wada and H. Ohno, *SAE Int. J. Fuels Lubr.*, 015, **8**(2), 454.
60. D. Ball, D. Moser, Y. Yang and D. Lewis, *SAE Int. J. Fuels Lubr.*, 2013, **6**(2), 450.

61. A. Fathali, Deactivation of Commercial Three-Way Catalysts: Experimental and Theoretical Studies, Doctoral Thesis, Department of Chemical and Biological Engineering, Chalmers University of Technology, Gothenburg, April 2014.
62. A. Fathali, F. Wallin, A. Kristoffersson and M. Laurell, *SAE Technical Paper*, 2015, 2015-01-1000, DOI: 10.4271/2015-01-1000.
63. D. Ball, C. Negohosian, D. Ross, D. Moser and R. McClaughry, *SAE Int. J. Engines*, 2013, **6**(4), 1922.
64. R. Moos, *SAE Int. J. Engines*, 2015, **8**(3), 1240.
65. A. Peters, *European Federation of Clean Air and Environmental Protection Associations (EFCA) International Symposium, Ultrafine Particles – Air Quality and Climate*, Brussels, May 4–5, 2015.
66. K. Lee, S. Choi and H. J. Seong, *DoE Annual Merit Review Meeting*, Washington DC, June 19, 2014.
67. H. J. Seong, *Hyundai Kia International Power Train Conference* 2015, Korea, October 27–28, 2015.
68. A. Maier, U. Klaus, A. Dreizler and H. Rottengruber, *SAE Int. J. Engines*, 2015, **8**(3), 1334.
69. J. Czerwinski, P. Comte, A. Wichser, A. Mayer, J. Lemaire, *SAE Technical Paper*, 2015, 2015-01-1079, DOI: 10.4271/2015-01-1079.
70. G. Karavalakis, *HEI Workshop*, December 2016.
71. W. Yinhui, Z. Rong, Q. Yanhong, P. Jianfei, L. Mengren, L. Jianrong, W. Yusheng, H. Min and S. Shijin, *Fuel*, 2016, **166**, 543.
72. T. W. Chan, M. Saffaripour, F. Liu, J. Hendren, K. A. Thomson, J. Kubsh, R. Brezny and G. Rideout, *Emiss. Control Sci. Technol.*, 2016, **2**, 75.
73. Y. Wen, Y. Wang, C. Fu, W. Deng, Z. Zhan, Y. Tang, X. Li and H. Ding, *SAE Technical Paper*, 2016, 2016-01-2284, DOI: 10.4271/2016-01-2284.
74. H. Badshah, D. Kittelson and W. Northrop, *SAE Int. J. Engines*, 2016, **9**(3), 1775.
75. T. Schmitz , S. Siemund, A. Siani, T. Neubauer and P. Burk, *Hyundai Kia International Power Train Conference* 2015, Korea, October 27–28, 2015.
76. H. J. Seong, *Hyundai Kia International Power Train Conference* 2015, Korea, October 27–28, 2015.
77. N. Zimmerman, J. M. Wang, C.-H. Jeong, M. Ramos, N. Hilker, R. M. Healy, K. Sabaliauskas, J. S. Wallace and G. J. Evans, *Environ. Sci. Technol.*, 2016, **50**, 2035, DOI: 10.1021/acs.est.5b04444.
78. M. Muñoz Fernandez and N. Heeb, *19th ETH-Conference on Combustion Generated Nanoparticles* June 28th–July 1st, 2015, Zurich.
79. *Combustion Generated Fine Carbonaceous Particles*, ed. H. Bockhorn, A. D'Anna, A. F. Sarofim, and H. Wang, ch. 9, Karlsruke University Press, 2009.
80. G. Karavalakis, D. Short, D. Vu, J. Yanf and T. Durbin, *SAE Powertrain, Fuels, and Lubes Conference*, Baltimore, October 2016.
81. J. Storey, M. DeBusk, S. Huff, S. Lewis, F. Li, J. Thomas and M. Eibl, *Health Effects Institute Workshop*, Chicago, December 8th 2016.

82. S. Zinola, S. Raux and M. Leblanc, *SAE Technical Paper*, 2016, 2016-01-2283, DOI: 10.4271/2016-01-2283.
83. T. W. Chan, E. Meloche, J. Kubsh, D. Rosenblatt, R. Brezny and G. Rideout, *SAE Int. J. Fuels Lubr.*, 2012, **5**(3), 1277.
84. UN International Panel on Climate Change, Climate Change 2013: The Physical Science Basis, Working Group I Contribution to the Fifth Assessment Report of the Intergovernmental Panel on Climate Change, Summary for Policymakers, Cambridge University Press.
85. T. W. Chan, E. Meloche, J. Kubsh and R. Brezny, *Environ. Sci. Technol.*, 2014, **48**, 6027.
86. C. Lambert, M. Bumbaroska, D. Dobson, J. Hangas, J. Pakko and P. Tennison, *SAE Int. J. Engines*, 2016, **9**, 1296.
87. A. Joshi, D. Bronfenbrenner, D. Rose, P. Nicolin, *15th Hyundai-Kia International Powertrain Conference*, 2015.
88. J. Richter, R. Klingman, S. Speiss and K. Wong, *SAE Int. J. Engines*, 2012, **5**(3), 1361.
89. B. Blakeman, *US Department of Energy Cross-Cut Lean Exhaust Emissions Reduction Simulations (CLEERS) Workshop*, April 2013, Dearborn.
90. D. Rose, T. Boger, R. Ingram-Ogunwumi, C. Bischof, *22nd Aachen Colloquium on Automobile and Engine Technology*, October 2013.
91. ''Umicore Update'', presentation at 16th Hyundai Kia International Powertrain Conference, Namyang, Korea, 2016.
92. C. Lambert, *CLEERS workshop*, April 2016.
93. N. Custer, C. Kamp, A. Sappok, J. Pakko, C. Lambert, C. Boerensen and V. Wong, *SAE Int. J. Engines*, 2016, **9**(3), 1604.
94. D. Rose, T. Boger, B. Coulet, P. Nicolin and F. Kunath, *16th Hyundai Kia International Powertrain Conference*, Namyang, Korea, 2016.
95. H. Seong, *CLEERS Workshop*, April 2016.
96. C. Morgan, *SAE Light-Duty Emissions Symposium*, Troy, MI, December 2014.
97. T. Schmitz, S. Siemund, A. Siani, T. Neubauer and P. Burk, *Hyundai Kia International Power Train Conference 2015*, Korea, October 27–28, 2015.
98. P. Nicolin, D. Rose, F. Kunath and T. Boger, *SAE Int. J. Engines*, 2015, **8**(3), 1253.
99. S. Philipp, R. Hoyer, F. Adam, S. Eckhoff, R. Wunsch, C. Schoen and G. Vent, *SAE Technical Paper*, 2013, 2013-01-1299, DOI: 10.4271/2013-01-1299.
100. J. Parks, T. Toops, J. Pihl and V. Prikhodko, *DoE Annual Merit Review Meeting*, Washington, DC, June 19, 2014.
101. V. Prikhodko, J. Parks, J. Pihl and T. Toops, *SAE Int. J. Engines*, 2016, **9**(2), 1289.
102. J. Parks, T. Toops, J. Pihl and V. Prikhodko, *DoE Annual Merit Review Meeting*, Washington, DC, June 2016.